

Comparative study on the electrochemical performance of PPY/GO binary and PPY-GO/ZnO ternary nanocomposites

G. Singh, Nisha, A. Kumar, H. Mudila*

Department of Chemistry, Lovely Professional University, Phagwara, Punjab-144411, India

Received: April 03, 2023; Revised: April 27, 2023

PPY/GO binary nanocomposites (PGs) and PPY-GO/ZnO ternary nanocomposites (PGZs) as electrode material were synthesized *via* the *ex-situ* method. The PGs, prepared by varying the proportions of GO (%w/w) in PPY, were characterized by FTIR, XRD, TGA, and electrochemical measurements. The PGs were analyzed by cyclic voltammetry (CV) for their electrochemical performance. The binary composite (PG5) having the highest specific capacitance ($C_s=391.3$ F/g) value was preferred for the preparation of ternary composites, i.e., PGZs with ZnO in different ratios (%w/w) by the *ex-situ* method. The highest specific capacitance of 352.1 F/g was obtained for PGZ-1 at 1 mV/s which is lower than for its binary counterpart (PG5) but was higher than those of ZnO, PPY, and GO. The incorporation of GO has enhanced the electrochemical performance of PGs, however, the encapsulation of ZnO in PG was found to decrease the electrochemical response of PGZs. The result suggested this to occur due to the disorder caused in the PPY chains by ZnO.

Keywords: Conducting polymer; Composites; Capacitance; Graphene oxide; Transition metal oxide, Clean energy.

INTRODUCTION

Conventional energy sources are largely employed to encounter the need for the energy required in various aspects of life. The use of these energy sources at a tremendous rate is the major contributor to climate changes such as air pollution, global warming, etc. [1]. To overcome these issues there is a great need to develop energy techniques that are readily available and environmentally friendly. Among the various energy sources, electrochemical supercapacitors are considered the potent candidates widely used in power inventors, electrochemical actuators, power supplies, etc. The mechanism of charge storage in supercapacitors is based on (a) electrochemical double-layer capacitors (EDLC) or (b) fast and reversible redox reactions that take place on the interface of electrodes and electrolytes (pseudo capacitors) [1, 2]. Various types of electroactive material, *viz.*, carbonaceous material, conducting polymers (CPs), and transition metal oxides (TMOs) are employed as the electrode material in supercapacitors. CPs are appropriate as an electrode because of their high porosity, storage ability, and reversibility but they lack cyclic stability and slow charging-discharging rate. These drawbacks can be improved by entering structural changes in CPs by hybridizing them with other electroactive materials [2-4]. CPs with carbonaceous material like graphene oxide (GO) show a synergetic effect and produce an electrode with high capacitance behavior [5].

TMOs having pseudo capacitive behavior act as a filler between the CPs and carbonaceous material that may improve the electrolyte-electrode interaction resulting in the fast diffusion of ions and hence improving the capacitive behavior of the electrode material [3, 6]. However, some studies show a decrease in performance with the addition of TMO in the matrix [4]. Nowadays a variety of CPs (polypyrrole, polyaniline, etc.) are hybridized with carbonaceous material (GO, rGO, etc.), and TMOs (ZnO, V_2O_5 , and others) to form ternary composites used in supercapacitors for the storage of the electrochemical energy [7, 8]. This work presents the fabrication of PPY/GO binary nanocomposites (PGs) and PPY-GO/ZnO ternary nanocomposites (PGZs). The as-fabricated PGs and PGZs were further studied for their electrochemical performance by cyclic voltammetry (CV).

MATERIALS AND METHODS

Materials

Monomer pyrrole (PY, >99%, Spectrochem), graphite powder, potassium permanganate ($KMnO_4$), sulfuric acid (H_2SO_4), hydrogen peroxide (H_2O_2), and hydrochloric acid (HCl) were acquired from Loba Chemie. Ferric chloride ($FeCl_3$), and PVDF (polyvinylidene fluoride) were from Sigma Aldrich, N-cetyl -N, N, N- trimethyl ammonium bromide (CTAB), and ascorbic acid were obtained from S D Fine Chem. Ltd.

* To whom all correspondence should be sent:
E-mail: harismudila@gmail.com

Preparation of polypyrrole (PPY) and graphene oxide (GO)

Polypyrrole (PPY) was prepared by the chemical oxidative polymerization method mentioned by Mudila *et al.* 2013 which involves the use of pyrrole monomer, CTAB surfactant solution, and freshly prepared oxidant solution of FeCl₃ [7]. The preparation of GO was carried out by the modified Hummers method as mentioned by Song *et al.* 2014 [9].

Preparation of polypyrrole/graphene oxide (PG) binary composites

The preparation of PPY/GO composite in different ratios (wt %, in mg) was carried out by the *ex-situ* method. Requisite amounts of PPY and GO were taken in ethanol (Table 1) followed by mechanical mixing through sonication for 30 minutes to acquire homogeneity. The resultant mixture was then dried in an oven at 60°C.

Table 1. Corresponding ratio, amount, and names of PPY and GO composites

Material	Ratio					
	1: ¼	1: ½	1: ¾	1: 1	1: 2	1: 3
PPY (mg)	100	100	100	100	100	100
GO (mg)	25	50	75	100	200	300
Composite Name (PG)	PG1	PG2	PG3	PG4	PG5	PG6

Preparation of PPY-GO/ZnO (PGZ) ternary composite

Like the method followed for preparation of PGs, the PGZ was prepared (Table 2) with requisite amounts of PPY/GO and ZnO.

Table 2. Corresponding ratio, amount, and codes of PG (PPY-GO) and ZnO composites

Material	Ratio					
	1: ¼	1: ½	1: ¾	1: 1	1: 2	1: 3
PPY/GO (mg)	100	100	100	100	100	100
ZnO (mg)	25	50	75	100	200	300
Composite name (PGZ)	PGZ 1	PGZ 2	PGZ 3	PGZ 4	PGZ 5	PGZ 6

Preparation of the working electrodes

Electroactive material (0.05 g), and graphite (0.005 g) were mixed with the binder solution

(PVDF in NMP, 5 g/dL), followed by ultrasonication for 30 minutes and then applied on 1 cm² area of stainless steel (304-SS) sheet which was allowed to dry in a vacuum oven for 2 hours at 100°C. This SS sheet with a mass thickness of ~0.01 g on its surface functions as a working electrode [1, 9].

RESULTS AND DISCUSSION

FTIR Spectra

FTIR spectra of the samples were recorded in the range of 400-4000 cm⁻¹ (Fig. 1 (a-e)). In the FTIR spectra of PPY the bands at 1631, 1543, and 1415 cm⁻¹ are due to stretching of C=N, C=C, and C-N bonds. A broad band at 3300-3500 cm⁻¹ is due to stretching of N-H bond. The bands at 1039 cm⁻¹, 1300 cm⁻¹ and 884 cm⁻¹ are due to in-plane and out-of-plane deformation of C-H, C-N and C-H bonds. (Fig. 1a) [10, 11]. In the case of GO, the band at 3272 cm⁻¹ corresponds to O-H stretching. The vibrations at 1714 and 1585 cm⁻¹ are due to the carbonyl (C=O) and aromatic C=C bonds, respectively. The bands due to stretching of epoxy (C-O-C) and alkoxy (C-O) take place at 1225 and 1045 cm⁻¹ (Fig. 1b) [9]. In the FTIR spectrum of PG (Fig. 1c), the peak due to C=O stretching appears at 1705 cm⁻¹ which has been shifted towards the lower wavenumber as compared to the same peak of GO. This shifting of the C=O peak may be due to interaction (H-bonding) between the carbonyl (C=O) group of GO and the N-H group of PPY. The bands at 2979 and 1038 cm⁻¹ are due to stretching of O-H and epoxy (C-O-C) bonds of GO. The peaks at 1558 and 1210 cm⁻¹ are ascribed to the C=C and C-N stretching of the PPY ring confirming the presence of PPY in PG composites [12, 13].

FTIR spectra of ZnO (Fig. 1d) show the vibrational mode of ZnO at 560 cm⁻¹ [14]. The FTIR spectra of the PGZ composite (Fig. 1e) reflect the characteristic peaks of its individual components with some shifting in peak positions and peak intensities. The peak at 1708 cm⁻¹ is due to C=O stretching. The shifting of the C=O peak in the case of PGZ may be due to interaction between the carbonyl (C=O) group of GO and the N-H group of PPY. The bands at 3126 and 1059 cm⁻¹ are due to stretching vibrations of O-H and epoxy (C-O-C) bonds of GO. The absorption bands at 1562 and 1130 cm⁻¹ are ascribed to the C=C and C-N stretching of the PPY ring which further confirms the presence of PPY in PGZ composites. The absorption band at 896 cm⁻¹ due to ZnO in PGZ suggests the presence of ZnO in composite material [3, 12-14].

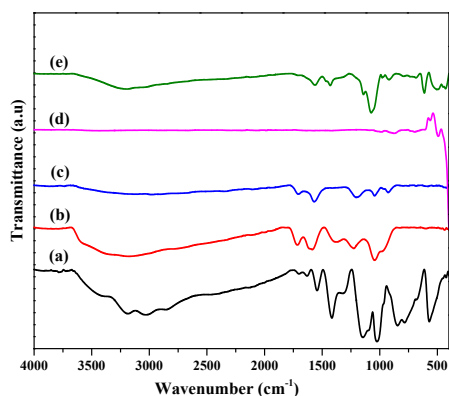


Fig. 1. FT-IR of (a) PPY, (b) GO and (c) PG (d) ZnO (e) PGZ

XRD spectra

The XRD spectra of graphite, PPY, GO, and PG are shown in Fig. 2 (a-f). The XRD spectra of PPY show a broad peak at $2\theta=27.52^\circ$ with interplanar spacing (d spacing) of 0.33 nm suggesting its amorphous nature (Fig. 2b) [4, 10]. The XRD pattern of graphite shows a sharp and intense peak at $2\theta=26.38^\circ$ with spacing (d=0.35 nm) indicating well-defined ordered arrangements of graphite layers (Fig. 2a). GO shows a peak at $2\theta = 10.91^\circ$ with d spacing 0.85 nm (Fig. 2c). The increase in the gallery spacing in case of GO as compared to graphite is ascribed to the encapsulation of oxygen moieties between the carbon layers of GO [7, 15]. The spectra of PG composites show two peaks at $2\theta = 11.89^\circ$ due to GO and $2\theta = 23.53^\circ$ due to PPY (Fig. 2d). These peaks signify the integration of GO layers over PPY amorphous nature of composites. [7, 12, 16]. In the XRD spectra of ZnO (Fig. 2e) the peaks at 31° , 34° , 36° , 47° , 56° , 63° and 72° signify its crystal behavior. In the XRD spectra of PGZ, Fig. 2f, the

peaks of PPY and GO are shifted and the intensity of the peaks increases with the increase of ZnO content suggesting an interaction between the three components in the composite material, which enhances the electrochemical stability of the ternary composite. [15, 17-19]

Thermal analysis

TGA curves of PPY, GO, PG, and PGZ are shown in Fig. 3 (a-e) below. Initially the weight loss at a temperature $< 100^\circ\text{C}$ is due to the removal of moisture content in the prepared samples. In case of PPY the weight loss starts at TG onset of 207°C with residual weight (W_r %) of 79.22. The weight loss of PPY continuously increases as the temperature rises and it ends at a TG offset of 595°C indicating the volatilization of PPY (Fig. 3a). In case of GO the weight loss takes place at TG onset 187°C with W_r % of 76.26 and ends at TG offset of 340°C . This loss is mainly due to the removal of oxygen functionalities from the surface of GO (Fig. 3b). [8, 12]. In PG the weight loss at $150\text{-}170^\circ\text{C}$ is probably due to the removal of oxygen-containing moieties. The major weight loss in PG after 230°C arises due to the degradation of PPY from the composite (Fig. 3c). [8, 20]. In the TGA curve of ZnO, the weight loss is due to the removal of moisture content (Fig. 3d) [14]. In case of PGZ, Fig. 3e, the weight loss at TG onset 212°C and 348°C is due to the removal of oxygen-containing functional groups and the degradation of the polymer chain from the surface of the composite material. The interaction between PPY and GO functionalities along with the barrier effects of ZnO imparts additional stability to the PGZ in comparison to PPY and GO [14, 21]

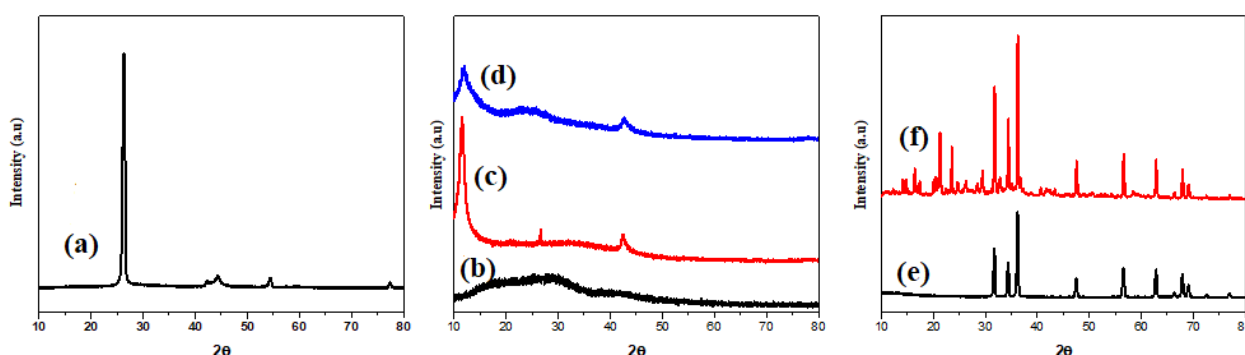


Fig. 2. XRD of (a) graphite (b) PPY, (c) GO (d) PG5 (e) ZnO (f) PGZ1

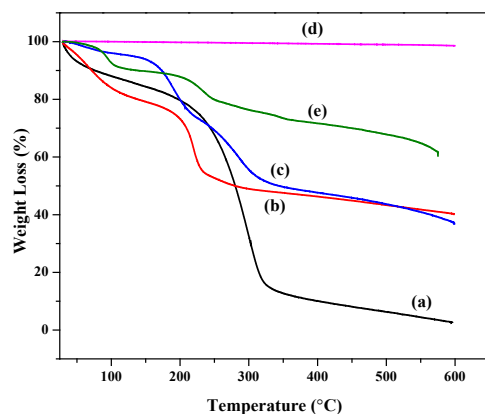


Fig. 3. TGA of (a) PPY (b) GO (c) PG5 (d) ZnO (e) PGZ1

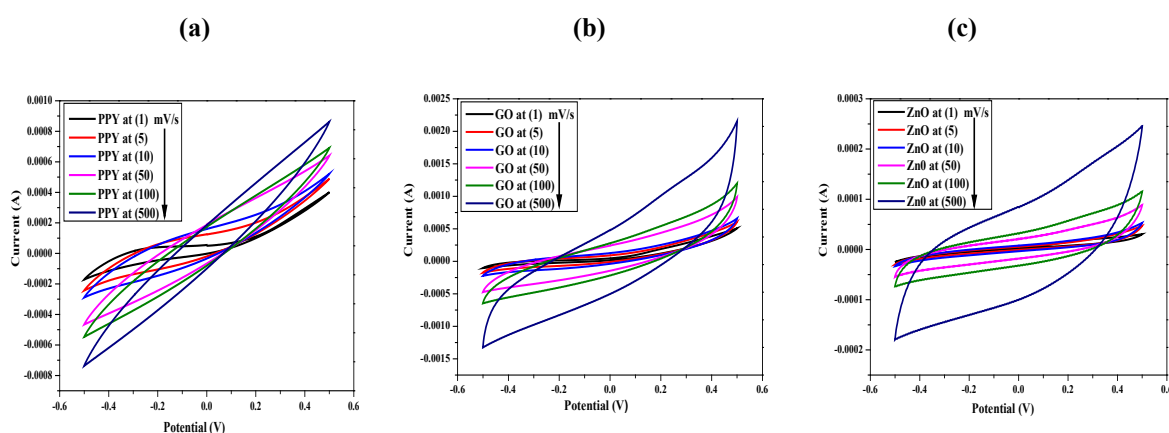


Fig. 4. CV curves of (a) PPY (b) GO (c) ZnO at different scans.

Table 3. Cs values of PPY, GO and ZnO at different scans

Scan mV/s	Cs Values		
	PPY	GO	ZnO
1	102.2	233.0	69.2
5	43.9	121.9	28.1
10	27.6	53.3	11.3
50	16.1	26.1	4.5
100	4.1	8.4	2.2
500	2.0	4.3	1.3

Electrochemical measurement of PPY, GO, and ZnO

ZnO, an *n*-type semiconductor, was found to have much lower Cs as compared to PPY and GO. This may be attributed to the bandgap of ZnO which has been reported to be higher (3.2 eV) as compared to PPY (3.0 eV) and GO (2.2 eV). This higher bandgap of ZnO probably reduces the chances of movement of an electron from the valence to the conduction band. Also, the chances of agglomeration in the case of ZnO can reduce the probability of higher Cs by reducing the surface area (Table 3). [22-23].

Electrochemical measurements

The CV curves of PPY, GO, ZnO, PGs, and PGZs were recorded within the potential window of -0.5 to 0.5V at different scan rates in 1 M KOH electrolytic solution as mentioned earlier [6, 12].

A regular increase in the peak current values with scan rates within the potential window for individual components i.e., PPY, GO, and ZnO, was observed [7]. The low Cs value of PPY is due to its compact structure which does not allow the diffusion of counter-ion readily into its internal matrix. GO gives higher Cs due to increased surface area, porous structure, and large interlayer gaps which makes the

diffusion more feasible as compared to the PPY chains [12, 22].

Electrochemical measurement of PGs

The C_s value of PGs increases with an increase in the amount (%w/w) of GO up to a certain limit and then decreases with the addition of GO in the composite material at all scans (Fig. 5a). This decrease may be due to the assemblage of GO layers with PPY on further addition of GO that results in the decrease of the active surface area of the composite and increase in the resistance that hindered the diffusion of ions on its surface. Therefore, the right amount of GO is necessary for composite material for the effective interaction between PPY and GO which facilitates the transport

of ions and decreases the resistance to the movement of ions during the charging/discharging process [24].

The C_s values of different PGs at different %w/w of GO are shown in Table 3 with the highest C_s value for PG5 (Fig. 4b). The C_s value of PG5 is higher than those of PPY, and GO which is because the introduction of GO into the PPY matrix increases the surface area and porosity of the composite material allowing the fast diffusion of counter-ions on its surface, and enhancing its electrochemical behavior [12, 22]. The slope, as well as the area of the CV curve of PGs is higher compared to PPY and GO suggesting the lower resistance < fast ion diffusion rate and good capacitance behavior in the composite material [6].

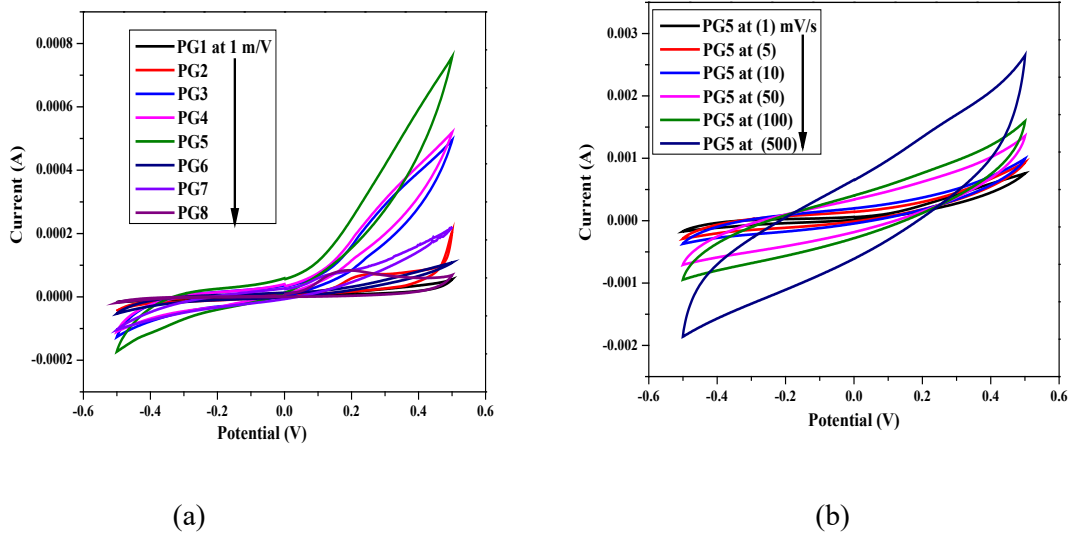


Fig. 5. CV curves of (a) PG with different %w/w of GO at 1 mV/S (b) PG5 at different scans.

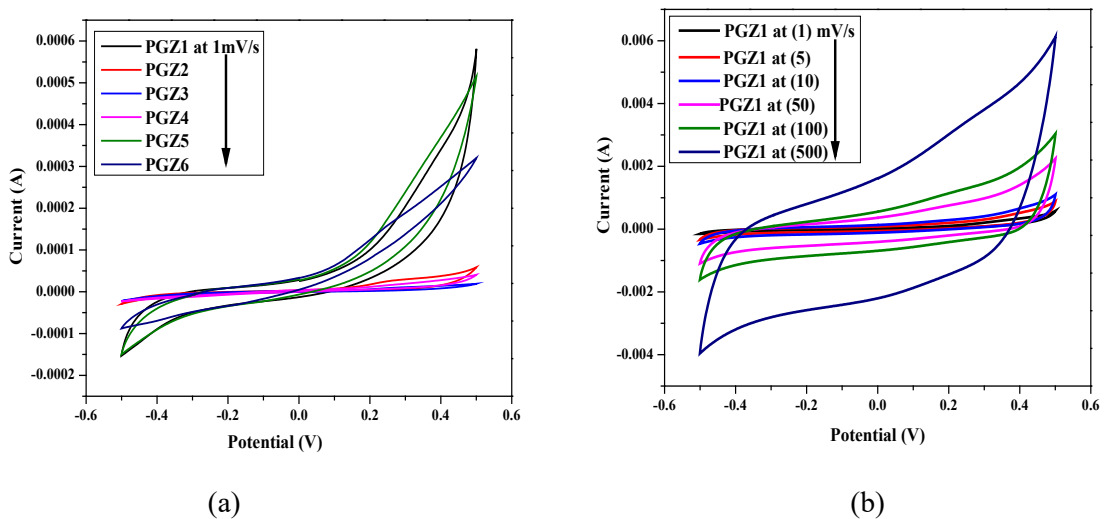


Fig. 6. CV curves of (a) PGZ with different %w/w of ZnO at 1 mV/S (b) PGZ1 at different scans.

Table 4. Cs values of PGs at different scans

Scan mV/s	Cs values (F/g)							
	PG1	PG2	PG3	PG4	PG5	PG6	PG7	PG8
1	245.8	264.5	295.1	330.1	391.3	311.5	276.9	241.4
5	78.2	87.2	95.1	120.3	137.6	101.6	89.3	76.3
10	52.2	65.2	69.6	83.1	98.1	71.0	69.1	51.1
50	23.9	29.4	33.1	35.1	42.3	32.3	23.4	24.2
100	6.5	10.3	12.0	13.4	27.2	9.6	9.3	6.5
500	4.1	6.4	7.1	8.5	10.0	6.8	7.1	3.9

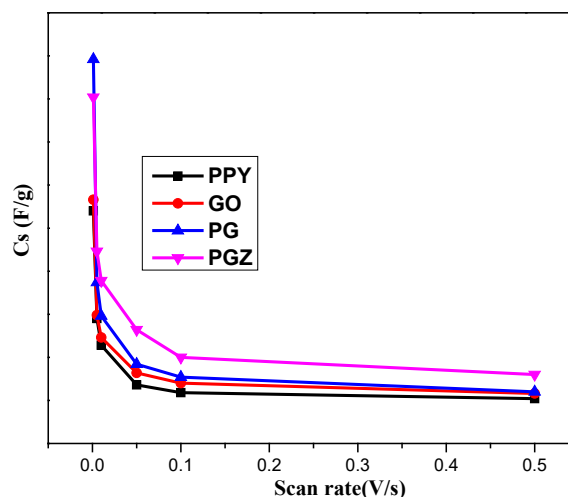
Table 5. Cs values of PGZs at different scans

Scan rate mV/s	Cs values (F/g)					
	PGZ1	PGZ2	PGZ3	PGZ4	PGZ5	PGZ6
1	352.1	256.5	182.4	47.5	26.3	18.9
5	137.5	121.3	59.9	16.3	10.5	13.5
10	94.5	89.3	38.1	12.6	8.6	7.4
50	39.0	32.3	13.5	8.2	4.4	4.2
100	25.1	21.1	8.3	7.3	3.6	3.1
500	9.4	9.1	3.4	3.8	2.7	2.2

Electrochemical measurement of PGZs

The Cs values of PGZ (Table 3) increase with an increase in the amount of ZnO up to a certain limit and then decrease with further addition of ZnO in the PG composite at a particular scan (Fig. 6a). This decrease may be due to the blockage of the porous surface of PG composite that results in the decrease of the active surface area of the ternary composite and an increase in the resistance that hinders the diffusion of ions on its surface. Thus, a requisite amount of ZnO is necessary for a composite material that decreases the internal resistance and enhances the electrochemical performance of the composite material [24].

The specific capacitance of PPY, GO, PGs, and PGZs decreases as the scan rate increases within a potential window, as shown in Fig. 7. High Cs value at a low scan rate is due to the fact that electrolyte ions have enough time to attach to the surface of the material resulting in their strong interaction with the active sites of the electrode material and hence, enhancing its capacitive behavior. At higher scan rates the rate of diffusion of ions in the electrolyte is fast but the number of ions on the active sites of the electrode decreases resulting in a decrease in their Cs values. The oxidation and reduction peaks due to the internal resistance of the electrode are shifted towards positive and negative potential, respectively, with an increase in scan rate [2, 6].

**Fig. 7.** Effect of scan rate on Cs value of PPY, GO, PG and PGZ

It is significant to note that the Cs of respective PGZs are lower as compared to the Cs of PGs. This relative decrease in the Cs in the case of PGZs may be attributed to the presence of ZnO which itself has a lower Cs due to the presence of a larger bandgap. The presence of ZnO in the matrix of PG brings undesired disorder in the PPY chain thus generating a large polaron bandgap as compared to the PG [4]. Further, it was also observed that with the increase in the amount of ZnO in the matrix of PG (specifically PG5) the Cs were found to get considerably lower (Table 5, Fig. 7).

CONCLUSIONS

A series of nanocomposites were fabricated by mixing PPY and GO (PGs) and PGs and ZnO (PGZs) in certain ratios. The obtained nanocomposites and individual materials were studied for their electrochemical behavior. CV of all the electroactive materials was taken for the earlier purpose, the CV results show that the PG5 was having the highest Cs (391.3 F/g) within all the PGs and individual components. With the addition of ZnO in PGZs, the Cs were found to decrease as compared to the parent PG5, possibly due to a large bandgap and low Cs of ZnO. Additionally, it was proposed that the ZnO may have generated disorder in the PPY chains again effectively reducing the Cs of PGZs. Out of all PGZs, PGZ1 was found to have the highest Cs (352.1 F/g) which continues to decrease with increasing ZnO in the PG matrix.

Conflicts of interest: The authors declared no conflicts of interest.

REFERENCES

1. A. Singh A. Chandra, *J. Appl. Electrochem*, **43**(8), 773 (2013).
2. P. Asen, S. Shahrokhian, A. Irajizad, *Int. J. Hydrog. Energy*, **42**(33), 21073 (2017)
3. A. Pruna, Q. Shao, M. Kamruzzaman, J. A Zapien, A. Ruotolo, *Electrochim. Acta*, **187**, 517 (2016).
4. S. Dey A. K. Kar, *J. Sol-Gel Sci. Technol.*, **102**, 679 (2021).
5. J. Guerrero-Contreras, F. Caballero-Briones. *Mater. Chem. Phys*, **153**, 209 (2015).
6. W. K. Chee, H. N. Lim, I. Harrison, K. F Chong, Z., Ng, C. H. Zainal, N. M. Huang, *Electrochim. Acta*, **157**, 88 (2015).
7. H. Mudila, M. G. H. Zaidi, S. Rana, V. Joshi, S. Alam. *Int. J. Anal. Chem.* **4**(3), 139 (2013).
8. H. Mudila, V. Joshi, S. Rana, M. G. H. Zaidi, S. Alam, *Carbon Lett.* **15**(3), 171 (2014).
9. J. Song, X. Wang, C. T. Chang. *J. Nanomater.*, **2014**, 1. (2014)
10. A. Bisht, R. Sati, K. Singhal, S. Mehtab, M.G.H. Zaidi, *Advances in Solar Power Generation and Energy Harvesting*, 127 (2020)
11. R. Rikhari, B. Saklani, A. Bisht, S. Mehtab, M.G.H. Zaidi, *Sens. Lett.*, **17**, 511 (2019)
12. S. Konwer, R., Boruah, S. K. Dolui. *J. Electron. Mater.*, **40**(11), 2248 (2011).
13. S. Kulandaivalu, N. Suhaimi, Y. Sulaiman, *Sci. Rep.*, **9**(1) (2019).
14. A. Batoool, F. Kanwal, M. Imran, T. Jamil, S. A. Siddiqi, *Synth. Met.*, **161** (23-24), 2753 (2012).
15. F. Yin, J., Ren, Y. Zhang, T. Tan, Z. Chen. *Nanoscale Res. Lett.*, **13**(1). (2018).
16. L. Li, K. Xia, L. Li, S. Shang, Q. Guo, G. Yan. *J. Nanopart. Res*, **14**(6) (2012).
17. A. Mostafaei, F. Nasirpouri, *Prog. Org. Coat.*, **77**(1), 146 (2014).
18. N. I. T. Ramli, S. A. Rashid, M. S. Mamat, Y. Sulaiman, S. A. Zobir, S. Krishna. *Electrochim. Acta*, **228**, 259 (2017).
19. P. Patil, G. Gaikwad, D. R. Patil, J. Naik, *Bull. Mater. Sci.*, **39**(3), 655 (2016).
20. S. Bose, T. Kuila, M. E. Uddin, N. H Kim, A. K. T., Lau, J. H. Lee, *Polymer*, **51**(25), 5921 (2010).
21. M. Ates, S. Caliskan, M. Gazi, *Fuller. Nanotub. Carbon Nanostructures*, **26**(10), 631 (2018).
22. P. Joshi, S. Mehtab, M.G.H Zaidi, *Bull. Chem. Soc. Jpn*, **95** (6), 855 (2022)
23. H. Lv, Y. Guo, Z. Yang, Y. Cheng, L.P. Wang, B. Zhang, Y. Zhao, Z. J. Xu, G. Ji, *J. Mater. Chem. C*, **5**(3), 491 (2017).
24. G. Liu, Y. Shi, L. Wang, Y. Song, S. Gao, D. Liu, L. Fan, *Carbon Lett*, **30**(4), 389 (2019).